

## Local Entanglement Entropy and Mutual Information across the Mott Transition in the Two-Dimensional Hubbard Model

C. Walsh,<sup>1</sup> P. Sémon,<sup>2</sup> D. Poulin,<sup>3,4</sup> G. Sordi,<sup>1,\*</sup> and A.-M. S. Tremblay<sup>3,4</sup>

<sup>1</sup>*Department of Physics, Royal Holloway, University of London, Egham, Surrey, United Kingdom, TW20 0EX*

<sup>2</sup>*Computational Science Initiative, Brookhaven National Laboratory, Upton, New York 11973-5000, USA*

<sup>3</sup>*Département de physique & Institut quantique, Université de Sherbrooke, Sherbrooke, Québec, Canada J1K 2R1*

<sup>4</sup>*Canadian Institute for Advanced Research, Toronto, Ontario, Canada, M5G 1Z8*



(Received 26 July 2018; published 11 February 2019)

Entanglement and information are powerful lenses to probe phase transitions in many-body systems. Motivated by recent cold atom experiments, which are now able to measure the corresponding information-theoretic quantities, we study the Mott transition in the half-filled two-dimensional Hubbard model using cellular dynamical mean-field theory, and focus on two key measures of quantum correlations: entanglement entropy and a measure of total mutual information. We show that they detect the first-order nature of the transition, the universality class of the end point, and the crossover emanating from the end point.

DOI: 10.1103/PhysRevLett.122.067203

**Introduction.**—The Mott transition is a metal-insulator transition caused by electron-electron interactions in a half-filled band [1,2]. As observed in a number of materials, it is a first-order transition that ends at finite temperature at a critical end point [2–9]. It plays a central role in the physics of quantum materials [2,10]. It is possible to explain this transition within the dynamical mean-field solution of the paradigmatic model of strongly correlated electrons, the Hubbard model [11]. That model can be mimicked accurately by ultracold atom experiments in optical lattices [12–15].

Recent experimental progress with single-atom microscopy has bridged quantum materials and quantum information by measuring both the thermodynamics and the information-theoretic entanglement of the Hubbard model [16,17]. We take advantage of these recent experimental advances to open a new window on the interaction-driven Mott transition at half-filling.

The Mott transition offers a unique opportunity to study information-theoretic measures of a first-order transition, from its quantum low temperature limit all the way to its finite-temperature critical end point and beyond. In the supercritical regime, crossover phenomena associated with the so-called Widom line [18–20] are expected. Information-theoretic measures have been used to probe quantum-critical points [21–25] or finite-temperature continuous transition [26] with the goal of understanding phases of matter as different structures of entanglement distribution in a system.

Motivated by recent experiments with ultracold atoms [17], we characterize the interaction-driven Mott transition in the two-dimensional Hubbard model using quantum-information measures, as generalized to fermions by Zanardi [27]. The entanglement entropy between a single site and the rest

of the system has emerged as a useful tool to characterize quantum phase transitions [23]. At finite temperatures however, both entanglement and thermal fluctuations contribute to the single-site entropy  $s_1$ , which is therefore no longer a measure of quantum entanglement only [28]. The difference  $\bar{I}_1 = s_1 - s$  between the local entropy  $s_1$  and the thermodynamic entropy  $s$  leads to a measure of total mutual information that captures both classical and quantum correlations between a site and its environment [29]. We demonstrate that both  $s_1$  and  $\bar{I}_1$  (a) pinpoint the first-order nature of the Mott transition by showing hysteretic behavior, (b) detect the universal critical exponents of the Mott end point, and (c) identify the crossovers emanating from the end point in the supercritical region by showing sharp variations marked by inflections.

Finite-temperature studies of information-theoretic measures of the Hubbard model have appeared, e.g., on the kagome lattice [30], but previous studies of the Mott transition focused on bosonic systems [16,31,32] or on fermionic systems at zero temperature [21,24,25,33].

**Model and method.**—We consider the single-band Hubbard model on the square lattice in two dimensions (2D)  $H = -\sum_{\langle ij \rangle \sigma} t_{ij} c_{i\sigma}^\dagger c_{j\sigma} + U \sum_i n_{i\uparrow} n_{i\downarrow} - \mu \sum_{i\sigma} n_{i\sigma}$ , where  $c_{i\sigma}^\dagger$  and  $c_{i\sigma}$  operators create or destroy an electron of spin  $\sigma$  on site  $i$ ,  $n_{i\sigma} = c_{i\sigma}^\dagger c_{i\sigma}$  is the number operator,  $t_{ij}$  is the nearest neighbor hopping,  $\mu$  is the chemical potential, and  $U$  the onsite Coulomb repulsion. We solve this model within plaquette cellular dynamical mean-field theory (CDMFT) [34–36], which is a cluster extension of dynamical mean-field theory (DMFT) [11]. The cluster in a bath problem is solved using the continuous-time quantum Monte Carlo method [37–39] based on the hybridization expansion of the impurity action (CT-HYB). Further details

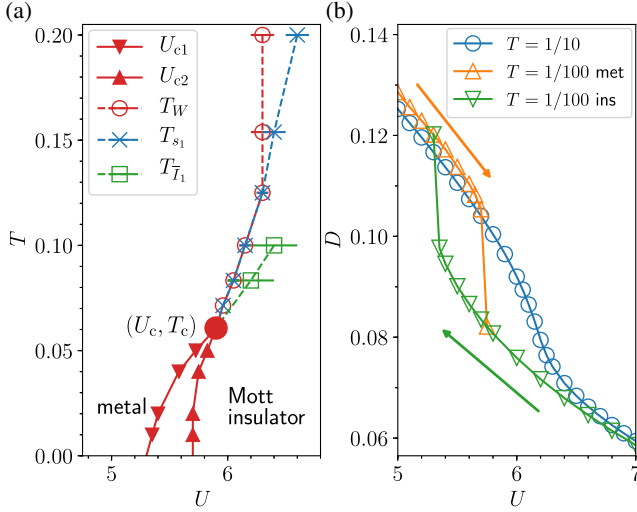


FIG. 1. (a) Temperature  $T$  versus interaction strength  $U$  phase diagram of the 2D Hubbard model at half filling ( $n = 1$ ) within plaquette CDMFT. Coexistence associated with the first-order transition between a metal and a Mott insulator terminates at the second-order critical end point  $(U_c, T_c)$ . From the end point emerges a crossover line (Widom line) defined by the maxima in the correlation length. Here we estimate the Widom line by the locus of the inflection point in the double occupancy  $D(U)_T$  at different temperatures (open red circles,  $T_W$ ). This line overlaps with the loci of the inflection points in the local entropy  $s_1(U)_T$  (blue crosses,  $T_{s_1}$ ) and in the total mutual information  $\bar{I}_1(U)_T = s_1 - s$  (green squares,  $T_{\bar{I}_1}$ ), where  $s$  is thermal entropy. (b) Double occupancy  $D$  versus  $U$  at  $n = 1$  and different temperatures. For  $T < T_c$ , hysteresis appears when sweeping  $U$  in the forward and reverse directions. Arrows show the sweep direction.

are in the companion article [40]. We work in units  $t = 1$ ,  $k_B = 1$ .

In the model that we study, the Mott transition is masked by long-range antiferromagnetic order. Nevertheless, introducing frustration decreases the antiferromagnetic transition temperature and can unmask the Mott transition [41,42]. A model with frustrated antiferromagnetism would lead to increased fermionic sign problems, so we stick with the simpler model. While it will not be possible to compare quantitatively our low-temperature results with experiments where antiferromagnetism is frustrated, we do not expect qualitative differences. In calculations we do not allow antiferromagnetic symmetry breaking, so the Mott transition extends all the way to zero temperature.

**Phase diagram.**—The temperature versus interaction strength phase diagram of the half-filled 2D Hubbard model obtained by CDMFT on a  $2 \times 2$  plaquette is known [43–45]. As shown in Fig. 1(a), at low  $T$  and finite  $U$ , the electron-electron correlations produce a first-order transition between a metal and a Mott insulator. This transition terminates in a second-order critical end point at  $(U_c, T_c)$ . From the end point emanates a crossover line, the Widom line, across which the correlation length peaks [18–20].

Near the end point, the loci of other response functions extrema converge into the Widom line [18,19]. Hence, the Widom line is a high-temperature precursor of the first-order Mott transition.

A convenient way to construct the  $T - U$  phase diagram of the half-filled model is to monitor the behavior of double occupancy  $D(U)_T$  [see Fig. 1(b)]. For  $T < T_c$ , hysteresis loops reveal the coexistence region  $U_{c1}(T) < U < U_{c2}(T)$  between metal and insulator. At  $T = T_c$  the coexistence region closes,  $D(U)$  is continuous with an infinite slope at  $U_c$ , and thermodynamic quantities such as double-occupancy fluctuations  $\partial D / \partial U$  diverge, thereby signaling a diverging correlation length. For  $T > T_c$ ,  $D(U)$  still shows an inflection point. We use the inflection point in  $D(U)_T$  to estimate the Widom line (see also companion article [40]).

The important aspect is that thermodynamic properties, from low temperature up to high temperature, are controlled by the transition and its associated supercritical crossover. Here we extend this connection to information-theoretic measures.

**Local entropy and entanglement entropy.**—The entropy of a subsystem  $A$  is defined as  $s_A = -\text{Tr}_A[\rho_A \ln \rho_A]$ , where the reduced density matrix  $\rho_A$  is obtained by tracing the complement  $B$  of  $A$  from the global density matrix,  $\rho_A = \text{Tr}_B[\rho_{AB}]$ . It is a measure of the lack of information, or uncertainty, in the state of  $A$ . At  $T = 0$ , this uncertainty is due to the entanglement between  $A$  and  $B$ , so  $s_A$  is called entanglement entropy. Here we focus on the local entanglement entropy [24,27], where  $A$  is a site of the lattice and  $B$  the remaining sites. The state space of a single site is spanned by  $\{|0\rangle, |\uparrow\rangle, |\downarrow\rangle, |\uparrow\downarrow\rangle\}$ . An important simplification occurs due to spin conservation, which ensures that the reduced density matrix is diagonal [27],  $\rho = \text{diag}(p_0, p_\uparrow, p_\downarrow, p_{\uparrow\downarrow})$ , where  $p_i$ , with  $i = \{0, \uparrow, \downarrow, \uparrow\downarrow\}$ , is the probability for a site to be empty, occupied with a spin up or down particle or doubly occupied. One has  $p_{\uparrow\downarrow} = \langle n_{i\uparrow} n_{i\downarrow} \rangle = D$ ,  $p_\uparrow = p_\downarrow = \langle n_{i\uparrow} - n_{i\downarrow} \rangle$ , and  $p_0 = 1 - 2p_\uparrow - p_{\uparrow\downarrow}$ . Thus  $s_1$  becomes  $s_1 = -\sum_i p_i \ln(p_i)$ , that can be easily calculated with CDMFT and measured in ultracold atom experiments [17]. For Hubbard-like Hamiltonians,  $s_1$  emerged as a useful tool to detect phase transitions and critical behavior, especially at  $T = 0$  where it measures entanglement [23–25, 33,46,47]. Our first contribution is to extend these studies to the first-order Mott transition from its low temperature quantum regime to the critical end point and supercritical crossovers, where  $s_1$  acquires thermal contributions and is no longer a measure of quantum entanglement only [28].

The local entropy  $s_1$  is shown as a function of  $U$  and different temperatures in Figs. 2(a), 2(b).  $s_1(U)$  monotonically decreases from a maximum value of  $\ln 4$  at  $U = 0$  to asymptotically reach the minimum value of  $\ln 2$  for  $U \rightarrow \infty$ . In these limits,  $\rho_A$  has equal populations in, respectively, four and two states. Physically,  $U$  suppresses the charge fluctuations and therefore the number of available states.

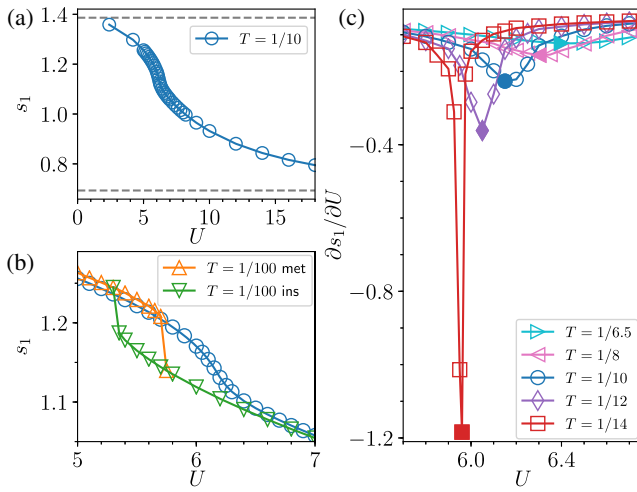


FIG. 2. (a) Local entropy  $s_1$  versus  $U$  at  $n = 1$  and  $T = 1/10$  (circles). Horizontal lines mark  $\ln 4$  (for  $U = 0$ ) and  $\ln 2$  (for  $U = \infty$ ). (b) Enlargement of  $s_1$  versus  $U$  at  $n = 1$  for  $T = 1/10$  and  $T = 1/100$  (triangles) close to the Mott transition. Inflection point for  $T > T_c$  and jumps for  $T < T_c$  are visible. (c) Increase in the slope  $\partial s_1 / \partial U$  as one approaches  $T_c$  from above. The positions of the minima are shown as blue crosses in Fig. 1(a).

In information theory language, a larger  $U$  leads to more knowledge about the site occupation, and hence to a decrease of its entropy.

Contrary to  $s$ , which is constrained to obey  $\partial s / \partial T > 0$  for reasons of thermodynamic stability,  $\partial s_1 / \partial T < 0$  is allowed. As can be seen by comparing the results for  $T = 1/100$  and  $T = 1/10$  in Fig. 2(b), this occurs on the metallic side because, at fixed filling, the number of available states on a single site can decrease when  $D(T)$  decreases with increasing  $T$ , a phenomenon which is known to occur at low  $T$  [11,48–50]. For  $T < T_c$ ,  $s_1(U)$  shows hysteresis loops at the Mott transition [see Fig. 2(b)], with  $(s_1)_{\text{ins}} < (s_1)_{\text{met}}$  since double occupancy is smaller in the insulating state. For  $T \geq T_c$ ,  $s_1(U)_T$  shows an inflection point. Approaching  $T_c$  from above, the first derivative  $\partial s_1 / \partial U$  becomes more negative and eventually tends to minus infinity at the Mott end point [see Fig. 2(c)]. This follows from  $(\partial s_1 / \partial D)(\partial D / \partial U)$  with  $\partial s_1 / \partial D$  regular and  $\partial D / \partial U \sim -|U - U_c|^{-1+1/\delta}$  with  $\delta > 1$  [39]. The locus of the inflection point of  $s(U)_T$  at different temperatures is shown in Fig. 1(a) and defines a crossover which is a precursor of the Mott transition in the supercritical region. Moreover, the asymptotic behavior of  $s_1(U)$  at  $T_c$  allows us to extract directly the critical exponent  $\delta$ . Although critical exponents are not generally observable in  $s_1$  [24], here this is possible since  $s_1$  depends only on double occupancy. The loci of the inflections of  $s_1(U)_T$  and of  $D(U)_T$  do not need to coincide in the supercritical region, they only need to converge towards each other at the critical end point. Surprisingly, inspection of Fig. 1(a) shows that the loci of inflections in  $s_1(U)_T$  and  $D(U)_T$  remain close, up to high temperature, suggesting an interesting connection between

fluctuations of the double occupancy,  $\partial D / \partial U$ , and variations in the entanglement entropy,  $\partial s_1 / \partial U$  [25]. Overall, these findings provide a strong link between thermodynamics and entanglement: the Mott transition, critical exponents, and associated high-temperature crossovers, can be determined solely from the local entropy  $s_1$ , without knowledge of the order parameter of the transition.

*Total mutual information.*—The mutual information  $I(A:B)$  captures the total correlations between two systems  $A$  and  $B$ . In particular, it takes value 0 if and only if the two systems are uncorrelated  $\rho_{AB} = \rho_A \otimes \rho_B$ . It is defined as  $I(A:B) = s_A + s_B - s_{AB}$ , and appears, for instance, in classical and quantum information theory [51,52].

Two complementary approaches are possible to investigate the behavior of mutual information at a phase transition in lattice systems. The first one aims to study the large scale behavior of the mutual information at the phase transition by scaling, i.e., by analyzing how the mutual information scales as a function of the volume of the system  $A$ . It has been shown in simple systems that the mutual information indeed shows critical scaling and subleading corrections to the area law [53] (according to which the mutual information scales at most proportionally to the size of the boundary separating  $A$  and  $B$  [54,55]). A second approach focuses instead on a single site and aims to study the behavior of the mutual information between a single site and its environment as a function of the tuning parameters of the phase transition.

Here, we follow the latter approach. As we shall see, advantages of this approach include simplicity of the calculations and the possibility of experimental confirmations with ultracold atoms. Specifically, we are interested in the mutual information between a given site  $i$  and the rest of the lattice, averaged over all sites. For the site labeled  $i = 1$ , we have  $I(1:\{> 1\}) = s_1 + s_{\{> 1\}} - s_{\{> 0\}}$  where we denote by  $\{> k\}$  the set of sites with indices greater than  $k$ , so  $\{> 0\}$  is the entire lattice. For the site labeled  $i = 2$ , the mutual information between  $i = 2$  and the rest of the lattice  $\{1\} \cup \{> 2\}$  would lead to double counting of the correlations between site 1 and 2, that have already been accounted for in the quantity  $I(1:\{> 1\})$ . To avoid such double counting, we trace over site 1, that has already been considered, and compute the mutual information between site 2 and the remaining sites  $\{> 2\}$ . Continuing this process, we define the total mutual information between a single site and the rest of the lattice as

$$\bar{I}_1 = \frac{1}{N} \sum_{i=1}^N I(i:\{> i\}) = \frac{1}{N} \sum_{i=1}^N (s_1(i) + s_{\{> i\}} - s_{\{> i-1\}}). \quad (1)$$

It is easy to see from this last form that most terms cancel, leaving  $\bar{I}_1 = (\sum_{i=1}^N s_1(i) / N - s)$ , where  $s$  is the thermodynamic entropy, defined as the entropy of the entire lattice divided by the number of sites. For a translationally invariant

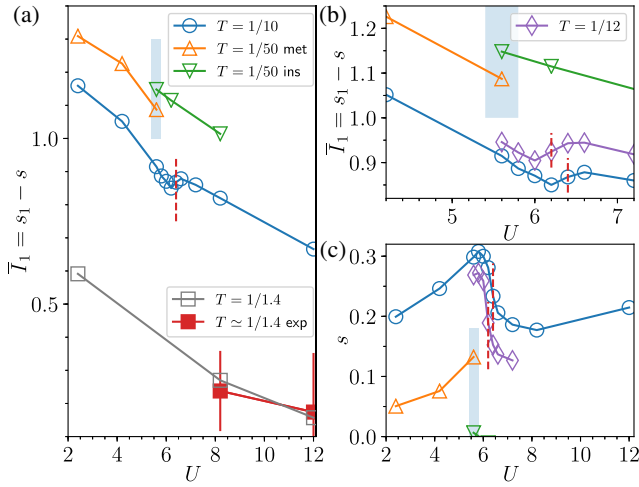


FIG. 3. (a) Total mutual information  $\bar{I}_1$  versus  $U$  at  $n = 1$  for different temperatures. Filled squares are experimental data of ultracold atoms in Ref. [17] at  $T \approx 1/1.4$  (see also Supplemental Material [56]). (b) Enlargement of panel (a) showing  $T = 1/10$ ,  $1/12$ , and  $T = 1/50$ . (c) Thermodynamic entropy  $s$  versus  $U$  at  $n = 1$  for the same temperatures of panel (b). In all panels, a dashed vertical line marks the inflection point while the shaded area marks the coexistence between metal and insulator. The loci of the inflections in  $\bar{I}_1(U)_T$  are shown as green squares in Fig. 1(a).

system, all  $s_1(i)$  are equal, so the total mutual information further simplifies to the difference between the local entropy and the thermodynamic entropy  $\bar{I}_1 = s_1 - s$ . This is the quantity studied in Ref. [17]. Contrary to the usual measure of mutual information, it is not equal to  $2s_1$  at zero temperature.

Figure 3(a) shows  $\bar{I}_1$  as a function of  $U$  and different temperatures (open symbols). The thermodynamic entropy  $s(U)$  is shown in Fig. 3(c) and discussed in the companion article [40]. Far from the Mott transition, Fig. 3(a) for  $\bar{I}_1$  shows that we find quantitative consistency with experimental data at higher temperature (filled squares; see also Supplemental Material [56]). At lower temperature,  $\bar{I}_1$  at weak interaction is larger than  $\bar{I}_1$  at strong interaction, because for weaker interaction the states are more extended; hence the density matrix does not factor in position space. Nevertheless  $\bar{I}_1$  can be quite large in the Mott insulator. At finite  $U$  electrons are localized, but their spins lock into singlet states due to the superexchange mechanism [43,45,57]. Hence they are correlated and  $\bar{I}_1$  cannot be zero. That is a basic message of the CDMFT: localization along with short-range correlations are key ingredients of the Mott transition, and this remarkably shows up in  $\bar{I}_1$ .

Consider now the vicinity of the Mott transition. For  $T < T_c$ ,  $\bar{I}_1$  shows hysteresis [triangles in Fig. 3(a)]. Although  $s_1$  is larger in the metal than in the insulator [Fig. 2(b)], the entropy  $s$  of the insulator is much smaller than that of the metal [Fig. 3(c)], leading to  $(\bar{I}_1)_{\text{met}} < (\bar{I}_1)_{\text{ins}}$

across the Mott transition. The latter inequality seems counterintuitive, but may be understood as follows: while local charge correlations are stronger in a delocalized conducting state, a localized insulating state leads to a stronger superexchange coupling, which results in increased spin correlations that overwhelm the loss of charge correlations [43,45,57]. For  $T \geq T_c$  [circles and diamonds in Figs. 3(a),(b)],  $\bar{I}_1$  displays nonmonotonic behavior: there is a local minimum that comes from the displacement of the local minimum in  $-s$  [Fig. 3(c)] caused by the monotonic decrease of  $s_1(U)$ . The rapid increase beyond the minimum reflects the steep slopes in  $s(U)$  and  $s_1(U)$ , marked by inflections (vertical red dashed lines), that eventually become infinite at  $(U_c, T_c)$  since both quantities scale as  $-\text{sgn}(U - U_c)|U - U_c|^{1/\delta}$ . For the Ising universality class, to which the Mott transition belongs,  $\bar{I}_1$  scales the same way  $\bar{I}_1 \sim \text{sgn}(U - U_c)|U - U_c|^{1/\delta}$  [40]. The locus of the inflection marking the most rapid increase of  $\bar{I}_1(U)_T$  at different temperatures defines the crossover line  $T_{\bar{I}_1}$  in the  $T - U$  phase diagram [see squares in Fig. 1(a)]. Therefore,  $\bar{I}_1$  detects the Mott transition, its supercritical crossover, and critical exponent at the Mott end point.

*Conclusion.*—We have characterized the Mott transition in the 2D Hubbard model with CDMFT using information-theoretic measures. The local entropy  $s_1$  and the total mutual information  $\bar{I}_1$  both detect the first-order nature of the transition, the criticality of the Mott end point, and the supercritical crossover. Our results are consistent with ultracold atom experiments of Ref. [17] and provide specific predictions for information-theoretic measures in the low-temperature region that may soon be accessible.

In highly frustrated optical lattices, such as the triangular lattice, one can, in principle, measure  $s_1$  and  $\bar{I}_1$  across the Mott transition and its supercritical crossover. One could thus verify our predictions of sharp variations of these quantities as a function of  $U$ , characterized by inflection points (above  $T_c$ ) and by hysteresis (below  $T_c$ ).

At the theory level, our information-theoretic description of a first-order transition from its quantum low temperature limit ( $T \ll T_c$ ), to its finite-temperature critical end point (at  $T_c$ ), and further on in the supercritical region ( $T > T_c$ ) offers a new kind of “criticality” [45,57], where strong variation of entanglement properties are not associated with a quantum critical point between ordered phases, but by proximity to a critical end point. Our finding of a deep link between the behavior of information-theoretic measures and of thermodynamic quantities can be extended to other first-order transitions ending in a critical end point, such as those found in electron systems [20,40,45,57], in spin systems [26,58], and quark matter [59].

We acknowledge Janet Anders and Marcelo Rozenberg for useful discussions. This work has been supported by the Natural Sciences and Engineering Research Council of

Canada (NSERC) under Grants No. RGPIN-2014-04584, No. RGPIN-2014-06630, the Canada First Research Excellence Fund and by the Research Chair in the Theory of Quantum Materials. Simulations were performed on computers provided by the Canadian Foundation for Innovation, the Ministère de l'Éducation des Loisirs et du Sport (Québec), Calcul Québec, and Compute Canada.

\*Corresponding author.

giovanni.sordi@rhul.ac.uk

- [1] N. F. Mott, *Metal-Insulator Transitions* (Taylor & Francis, London, 1974).
- [2] M. Imada, A. Fujimori, and Y. Tokura, Metal-insulator transitions, *Rev. Mod. Phys.* **70**, 1039 (1998).
- [3] D. B. McWhan, J. P. Remeika, T. M. Rice, W. F. Brinkman, J. P. Maita, and A. Menth, Electronic Specific Heat of Metallic Ti-Doped  $V_2O_3$ , *Phys. Rev. Lett.* **27**, 941 (1971).
- [4] P. Limelette, A. Georges, D. Jerome, P. Wzietek, P. Metcalf, and J. M. Honig, Universality and critical behavior at the Mott transition, *Science* **302**, 89 (2003).
- [5] M. Matsuura, H. Hiraka, K. Yamada, and Y. Endoh, Magnetic phase diagram and metal-insulator transition of  $NiS_{2-x}Se_x$ , *J. Phys. Soc. Jpn.* **69**, 1503 (2000).
- [6] K. Kanoda, Electron correlation, metal-insulator transition and superconductivity in quasi-2D organic systems,  $(ET)_2X$ , *Physica (Amsterdam)* **282C-287C**, 299 (1997), materials and mechanisms of superconductivity high temperature superconductors V.
- [7] S. Lefebvre, P. Wzietek, S. Brown, C. Bourbonnais, D. Jérôme, C. Mézière, M. Fourmigué, and P. Batail, Mott Transition, Antiferromagnetism, and Unconventional Superconductivity in Layered Organic Superconductors, *Phys. Rev. Lett.* **85**, 5420 (2000).
- [8] B. J. Powell and R. H. McKenzie, Quantum frustration in organic Mott insulators: From spin liquids to unconventional superconductors, *Rep. Prog. Phys.* **74**, 056501 (2011).
- [9] T. Furukawa, K. Kobashi, Y. Kurosaki, K. Miyagawa, and K. Kanoda, Quasi-continuous transition from a Fermi liquid to a spin liquid in  $\kappa$ -( $ET$ ) $_2$ Cu $_2$ (CN) $_3$ , *Nat. Commun.* **9**, 307 (2018).
- [10] P. W. Anderson, The resonating valence bond state in  $La_2CuO_4$  and superconductivity, *Science* **235**, 1196 (1987).
- [11] A. Georges, G. Kotliar, W. Krauth, and M. J. Rozenberg, Dynamical mean-field theory of strongly correlated fermion systems and the limit of infinite dimensions, *Rev. Mod. Phys.* **68**, 13 (1996).
- [12] R. Jordens, N. Strohmaier, K. Gunter, H. Moritz, and T. Esslinger, A Mott insulator of fermionic atoms in an optical lattice, *Nature (London)* **455**, 204 (2008).
- [13] U. Schneider, L. Hackermüller, S. Will, Th. Best, I. Bloch, T. A. Costi, R. W. Helmes, D. Rasch, and A. Rosch, Metallic and insulating phases of repulsively interacting fermions in a 3D optical lattice, *Science* **322**, 1520 (2008).
- [14] C. Hofrichter, L. Riegger, F. Scazza, M. Höfer, D. Rio Fernandes, I. Bloch, and S. Fölling, Direct Probing of the Mott Crossover in the  $SU(N)$  Fermi-Hubbard Model, *Phys. Rev. X* **6**, 021030 (2016).
- [15] E. Cocchi, L. A. Miller, J. H. Drewes, M. Koschorreck, D. Pertot, F. Brennecke, and M. Köhl, Equation of State of the Two-Dimensional Hubbard Model, *Phys. Rev. Lett.* **116**, 175301 (2016).
- [16] R. Islam, R. Ma, P. M. Preiss, M. E. Tai, A. Lukin, M. Rispoli, and M. Greiner, Measuring entanglement entropy in a quantum many-body system, *Nature (London)* **528**, 77 (2015).
- [17] E. Cocchi, L. A. Miller, J. H. Drewes, C. F. Chan, D. Pertot, F. Brennecke, and M. Köhl, Measuring Entropy and Short-Range Correlations in the Two-Dimensional Hubbard Model, *Phys. Rev. X* **7**, 031025 (2017).
- [18] L. Xu, P. Kumar, S. V. Buldyrev, S.-H. Chen, P. H. Poole, F. Sciortino, and H. E. Stanley, Relation between the Widom line and the dynamic crossover in systems with a liquid liquid phase transition, *Proc. Natl. Acad. Sci. U.S.A.* **102**, 16558 (2005).
- [19] P. F. McMillan and H. E. Stanley, Fluid phases: Going supercritical, *Nat. Phys.* **6**, 479 (2010).
- [20] G. Sordi, P. Sémon, K. Haule, and A.-M. S. Tremblay, Pseudogap temperature as a Widom line in doped Mott insulators, *Sci. Rep.* **2**, 547 (2012).
- [21] A. Anfossi, P. Giorda, A. Montorsi, and F. Traversa, Two-Point Versus Multipartite Entanglement in Quantum Phase Transitions, *Phys. Rev. Lett.* **95**, 056402 (2005).
- [22] L. Amico and D. Patanè, Entanglement crossover close to a quantum critical point, *Europhys. Lett.* **77**, 17001 (2007).
- [23] L. Amico, R. Fazio, A. Osterloh, and V. Vedral, Entanglement in many-body systems, *Rev. Mod. Phys.* **80**, 517 (2008).
- [24] D. Larsson and H. Johannesson, Single-site entanglement of fermions at a quantum phase transition, *Phys. Rev. A* **73**, 042320 (2006).
- [25] D. Larsson and H. Johannesson, Entanglement Scaling in the One-Dimensional Hubbard Model at Criticality, *Phys. Rev. Lett.* **95**, 196406 (2005).
- [26] J. Wilms, M. Troyer, and F. Verstraete, Mutual information in classical spin models, *J. Stat. Mech.* (2011) P10011.
- [27] P. Zanardi, Quantum entanglement in fermionic lattices, *Phys. Rev. A* **65**, 042101 (2002).
- [28] J. Cardy and C. P. Herzog, Universal Thermal Corrections to Single Interval Entanglement Entropy for Two Dimensional Conformal Field Theories, *Phys. Rev. Lett.* **112**, 171603 (2014).
- [29] B. Groisman, S. Popescu, and A. Winter, Quantum, classical, and total amount of correlations in a quantum state, *Phys. Rev. A* **72**, 032317 (2005).
- [30] M. Udagawa and Y. Motome, Entanglement spectrum in cluster dynamical mean-field theory, *J. Stat. Mech.* (2015) P01016.
- [31] A. M. Läuchli and C. Kollath, Spreading of correlations and entanglement after a quench in the one-dimensional Bose-Hubbard model, *J. Stat. Mech.* (2008) P05018.
- [32] I. Frérot and T. Roscilde, Entanglement Entropy Across the Superfluid-Insulator Transition: A Signature of Bosonic Criticality, *Phys. Rev. Lett.* **116**, 190401 (2016).
- [33] K. Byczuk, J. Kuneš, W. Hofstetter, and D. Vollhardt, Quantification of Correlations in Quantum Many-Particle Systems, *Phys. Rev. Lett.* **108**, 087004 (2012).
- [34] T. Maier, M. Jarrell, T. Pruschke, and M. H. Hettler, Quantum cluster theories, *Rev. Mod. Phys.* **77**, 1027 (2005).

- [35] G. Kotliar, S. Y. Savrasov, K. Haule, V. S. Oudovenko, O. Parcollet, and C. A. Marianetti, Electronic structure calculations with dynamical mean-field theory, *Rev. Mod. Phys.* **78**, 865 (2006).
- [36] A.-M. S. Tremblay, B. Kyung, and D. Sénéchal, Pseudogap and high-temperature superconductivity from weak to strong coupling. Towards a quantitative theory, *Low Temp. Phys.* **32**, 424 (2006).
- [37] E. Gull, A. J. Millis, A. I. Lichtenstein, A. N. Rubtsov, M. Troyer, and P. Werner, Continuous-time Monte Carlo methods for quantum impurity models, *Rev. Mod. Phys.* **83**, 349 (2011).
- [38] P. Sémon, C.-H. Yee, K. Haule, and A.-M. S. Tremblay, Lazy skip-lists: An algorithm for fast hybridization-expansion quantum Monte Carlo, *Phys. Rev. B* **90**, 075149 (2014).
- [39] P. Sémon and A.-M. S. Tremblay, Importance of subleading corrections for the Mott critical point, *Phys. Rev. B* **85**, 201101 (2012).
- [40] C. Walsh, P. Sémon, D. Poulin, G. Sordi, and A.-M. S. Tremblay, Thermodynamic and Information-Theoretic Description of the Mott Transition in the Two-Dimensional Hubbard Model, *Phys. Rev. B* **99**, 075122 (2019).
- [41] L. Fratino, P. Sémon, M. Charlebois, G. Sordi, and A.-M. S. Tremblay, Signatures of the Mott transition in the antiferromagnetic state of the two-dimensional Hubbard model, *Phys. Rev. B* **95**, 235109 (2017).
- [42] L. Fratino, M. Charlebois, P. Sémon, G. Sordi, and A.-M. S. Tremblay, Effects of interaction strength, doping, and frustration on the antiferromagnetic phase of the two-dimensional Hubbard model, *Phys. Rev. B* **96**, 241109 (2017).
- [43] H. Park, K. Haule, and G. Kotliar, Cluster Dynamical Mean Field Theory of the Mott Transition, *Phys. Rev. Lett.* **101**, 186403 (2008).
- [44] M. Balzer, B. Kyung, D. Sénéchal, A.-M. S. Tremblay, and M. Potthoff, First-order Mott transition at zero temperature in two dimensions: Variational plaquette study, *Europhys. Lett.* **85**, 17002 (2009).
- [45] G. Sordi, K. Haule, and A.-M. S. Tremblay, Mott physics and first-order transition between two metals in the normal-state phase diagram of the two-dimensional Hubbard model, *Phys. Rev. B* **84**, 075161 (2011).
- [46] S.-J. Gu, S.-S. Deng, Y.-Q. Li, and H.-Q. Lin, Entanglement and Quantum Phase Transition in the Extended Hubbard Model, *Phys. Rev. Lett.* **93**, 086402 (2004).
- [47] L. Campos Venuti, C. Degli Esposti Boschi, M. Roncaglia, and A. Scaramucci, Local measures of entanglement and critical exponents at quantum phase transitions, *Phys. Rev. A* **73**, 010303 (2006).
- [48] F. Werner, O. Parcollet, A. Georges, and S. R. Hassan, Interaction-Induced Adiabatic Cooling and Antiferromagnetism of Cold Fermions in Optical Lattices, *Phys. Rev. Lett.* **95**, 056401 (2005).
- [49] A.-M. Daré, L. Raymond, G. Albinet, and A.-M. S. Tremblay, Interaction-induced adiabatic cooling for antiferromagnetism in optical lattices, *Phys. Rev. B* **76**, 064402 (2007).
- [50] T. Paiva, R. Scalettar, M. Randeria, and N. Trivedi, Fermions in 2d Optical Lattices: Temperature and Entropy Scales for Observing Antiferromagnetism and Superfluidity, *Phys. Rev. Lett.* **104**, 066406 (2010).
- [51] T. M. Cover and J. A. Thomas, *Elements of Information Theory*, Wiley Series in Telecommunications and Signal Processing (Wiley-Interscience, New York, 2006).
- [52] J. Watrous, *The Theory of Quantum Information* (Cambridge University Press, Cambridge, England, 2018).
- [53] R. R. P. Singh, M. B. Hastings, A. B. Kallin, and R. G. Melko, Finite-Temperature Critical Behavior of Mutual Information, *Phys. Rev. Lett.* **106**, 135701 (2011).
- [54] M. M. Wolf, F. Verstraete, M. B. Hastings, and J. I. Cirac, Area Laws in Quantum Systems: Mutual Information and Correlations, *Phys. Rev. Lett.* **100**, 070502 (2008).
- [55] J. Eisert, M. Cramer, and M. B. Plenio, Colloquium: Area laws for the entanglement entropy, *Rev. Mod. Phys.* **82**, 277 (2010).
- [56] See Supplemental Material at <http://link.aps.org/supplemental/10.1103/PhysRevLett.122.067203> for a comparison with experiments of Ref. [17].
- [57] G. Sordi, K. Haule, and A.-M. S. Tremblay, Finite Doping Signatures of the Mott Transition in the Two-Dimensional Hubbard Model, *Phys. Rev. Lett.* **104**, 226402 (2010).
- [58] J. Iaconis, S. Inglis, A. B. Kallin, and R. G. Melko, Detecting classical phase transitions with Renyi mutual information, *Phys. Rev. B* **87**, 195134 (2013).
- [59] J. Knaute and B. Kämpfer, Holographic entanglement entropy in the qcd phase diagram with a critical point, *Phys. Rev. D* **96**, 106003 (2017).